

**ECONOMIC GEOLOGY
RESEARCH UNIT**

University of the Witwatersrand
Johannesburg

— . —

**THE ALBERT SILVER MINE REVISITED:
TOWARDS A MODEL FOR POLYMETALLIC
MINERALIZATION IN GRANITES OF THE BUSHVELD
COMPLEX, SOUTH AFRICA**

L.J. ROBB, V.M. ROBB and F. WALRAVEN

• INFORMATION CIRCULAR No. 277

UNIVERSITY OF THE WITWATERSRAND
JOHANNESBURG

**THE ALBERT SILVER MINE REVISITED:
TOWARDS A MODEL FOR POLYMETALLIC MINERALIZATION
IN GRANITES OF THE BUSHVELD COMPLEX,
SOUTH AFRICA**

by

L.J. ROBB¹, V.M. ROBB¹ AND F. WALRAVEN²

*(¹ Department of Geology, University of the Witwatersrand,
P/Bag 3, WITS 2050, South Africa*

*² Geological Survey of South Africa, P/Bag X112, Pretoria,
South Africa)*

**ECONOMIC GEOLOGY RESEARCH UNIT
INFORMATION CIRCULAR No. 277**

April, 1994

THE ALBERT SILVER MINE REVISITED: TOWARDS A MODEL FOR POLYMETALLIC MINERALIZATION IN GRANITES OF THE BUSHVELD COMPLEX, SOUTH AFRICA

ABSTRACT

The old Albert Silver Mine is a polymetallic deposit comprising concentrations of Cu-Pb-Zn-Ag-U-F within a set of sub-parallel quartz-hematite veins and occurring in the fine-grained apical phase of the 2050 Ma old A-type Bushveld granites. Mineralization occurs as an early pyrite-chalcopyrite-arsenopyrite-galena-sphalerite-(argentiferous) tetrahedrite paragenesis followed by a later, more oxidized assemblage comprising chlorite-hematite-fluorite-pitchblende. Accumulation of metals appears to have taken place at the interface between a coarse-grained porphyritic granite and an overlying fine-grained phase: veins occur in the latter and represent leakage of magmatic fluids from the differentiated, water-saturated, subjacent granite.

Mineralization processes in the Bushveld granites are believed to be related to long-lived circulation of dominantly magmatic fluids stimulated by the high heat productive capacity of the host rocks. Endo- and exogranitic tin-tungsten and base metal mineralization formed during an evolving hydrothermal system that lasted for several hundred million years, forming innumerable small-to-medium scale polymetallic deposits. At the Albert Silver Mine, unroofing of the cover sequences at circa 1600-1700 Ma resulted in the incursion of lower-temperature, high fO_2 meteoric fluids which remobilized the earlier sulphides and introduced the paragenetically late U-F mineralization.

_____oOo_____

**THE ALBERT SILVER MINE REVISITED: TOWARDS A MODEL FOR
POLYMETALLIC MINERALIZATION IN GRANITES OF THE BUSHVELD
COMPLEX, SOUTH AFRICA**

CONTENTS

	Page
INTRODUCTION	1
HISTORICAL ASPECTS	1
GEOLOGICAL SETTING	3
PETROGRAPHY	3
Coarse-grained Porphyritic Granite (Nebo-type)	3
Fine-grained Porphyritic Granite (Klipkloof-type)	3
Mineralized Veins	6
Wall-rock Alteration Zones	
Borehole Intersections	7
GEOCHEMICAL CHARACTERISTICS OF HOST GRANITOIDS	8
ORE FLUID CHARACTERISTICS	14
RADIOGENIC ISOTOPE CHARACTERISTICS	16
DISCUSSION	18
Styles of Polymetallic Mineralization in the Bushveld Granites	18
Zaaipplaats Mine	20
Rooiberg Mine	20
Albert Silver/Speedwell Mines	21
Towards a General Model	22
ACKNOWLEDGEMENTS	23
REFERENCES	23

____oOo____

Published by Economic Geology Research Unit
Department of Geology
University of the Witwatersrand
1 Jan Smuts Avenue
Johannesburg
South Africa

ISBN 1 86838 110 2

THE ALBERT SILVER MINE REVISITED: TOWARDS A MODEL FOR POLYMETALLIC MINERALIZATION IN GRANITES OF THE BUSHVELD COMPLEX, SOUTH AFRICA

INTRODUCTION

The acid phase of the circa 2050 Ma Bushveld Complex (BC) contains numerous economic occurrences of tin and fluorite, and is also highly prospective with regards a wide-range of other metals including copper, zinc, tungsten, molybdenum, silver, gold, uranium, lead and rare earth elements. Innumerable prospects containing a variety of combinations of the above elements are known to occur over large areas of the Bushveld granite. With its markedly differentiated petrogenetic history, its obvious metal-specific character and its high-heat producing character, the Bushveld granites represent an obvious target for polymetallic ore bodies. Despite these characteristics, however, the level of exploration activity in this metallogenic province at the present time is minimal, probably because most of the mines are now closed and there are few cohesive metallogenic models which explain the highly variable pattern of mineralization in the region. The object of this paper is to re-examine the geology and ore-characteristics of the Albert Silver Mine (ASM), a long-defunct deposit which nevertheless preserves many of the characteristics of polymetallic mineralization styles within the Bushveld granites. An attempt is then made to incorporate the characteristics of the ASM with observations from the few other well-studied deposits (particularly Sn-W) in the region and to provide a conceptual model for polymetallic mineralization in the suite as a whole.

HISTORICAL ASPECTS

The Albert Silver Mine was discovered in 1885 and was mined continuously for approximately 14 years, and then intermittently until about 1910. It occurs on the farm Roodepoortjie 250 JR about 80 km west-northwest of Pretoria (Fig. 1). In more recent times exploration companies have held the mineral rights over the mine and have periodically re-examined the occurrence. Four boreholes were drilled in 1952 and a further 26 drilled in the period 1967-1969. A geophysical and geochemical survey was carried out over the deposit by the Geological Survey of South Africa and in 1970 an MSc dissertation was submitted to the University of Natal on the mineralogy and related geology of the occurrence (Champion, 1970). In 1956 scintillometer surveys showed, for the first time, that significant concentrations of uranium (up to $1\text{kg}\cdot\text{ton}^{-1}$) are associated with the base- and precious-metal lodes. In the period 1978-1980 the property was re-examined as a potential copper-silver-uranium prospect and a further five boreholes were drilled. Present ore reserves to a depth of 150m are estimated to be 1,2 million tons at $73\text{g}\cdot\text{ton}^{-1}$ Ag, 0,42% Cu, 0,27% Pb and 100ppm U_3O_8 , and the deposit is generally regarded as uneconomic in the present market climate. During its productive years the mine was high-graded producing an estimated 20 000 tons of ore grading $1,14\text{kg}\cdot\text{ton}^{-1}$ Ag and 10% Cu (Voet, 1981). Recent assays of dump material also report isolated samples up to $400\text{g}\cdot\text{ton}^{-1}$ Au and 0,48% Sb.

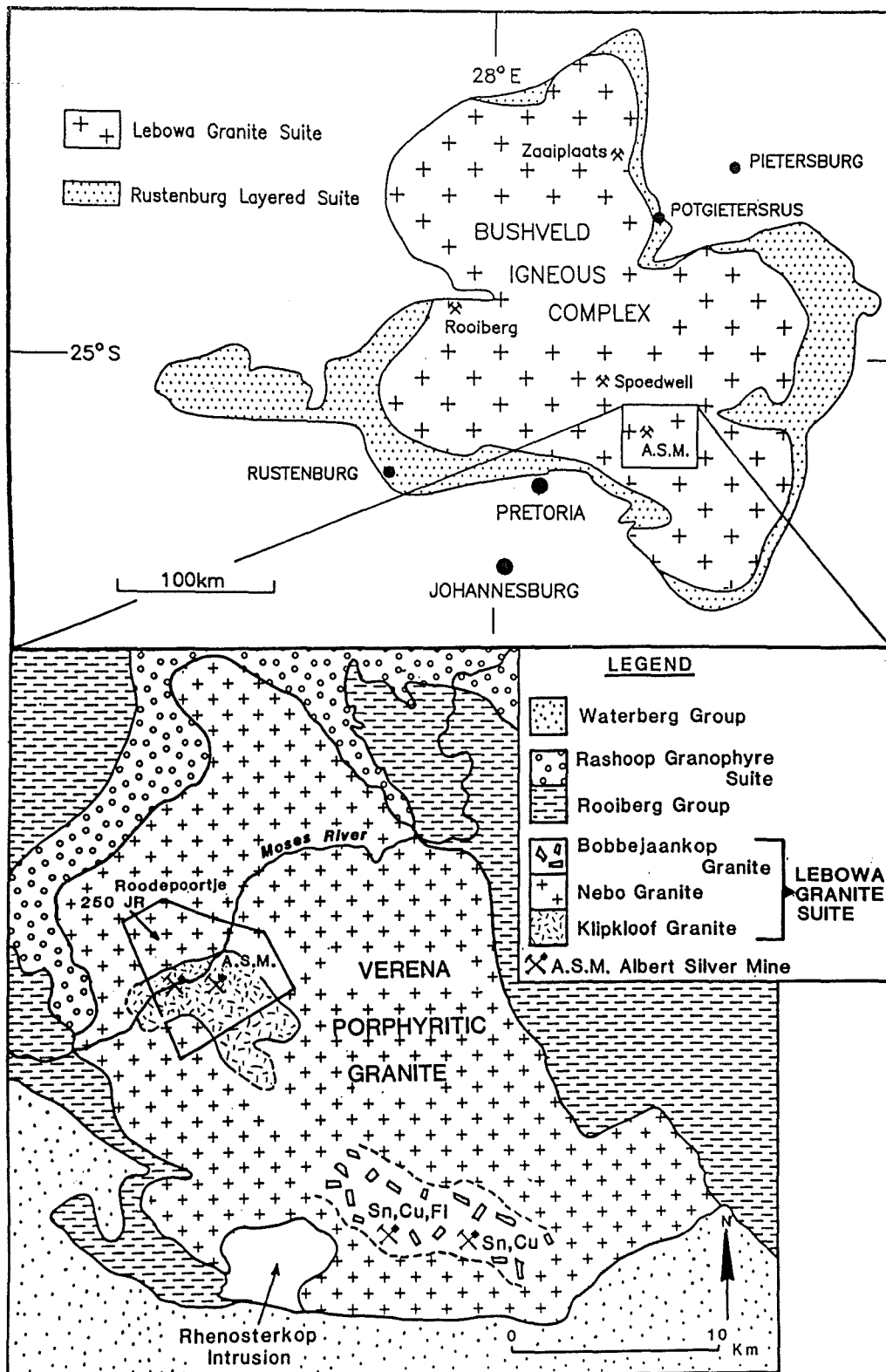


Figure 1: Locality map showing the location of Bushveld Complex ore deposits discussed in the text and the simplified geology around the Albert Silver Mine.

GEOLOGICAL SETTING

The Albert Silver Mine occurs in a segment of the Bushveld granite (Lebowa Granite Suite), known locally as the Verena Porphyritic Granite, which is bounded to the north by felsic volcanics of the Rooiberg Group and the Rashoop Granophyre Suite, and to the south by off-lapping sediments of the Waterberg Group (Fig. 1). The Verena Porphyritic Granite is typically very coarse grained, reddish, and markedly porphyritic, aspects which suggest that it represents a phase characteristic of the upper, more differentiated, portions of the generally sheet-like intrusion now referred to as the Nebo Granite. A schematic geological map of the Verena Porphyritic Granite and its position in relation to the extent of the BC is presented in Figure 1.

The ASM comprises an en echelon series of roughly east-west-trending quartz-hematite veins. All of these veins are hosted within a thin sheet of fine-grained porphyritic granite, which is texturally similiar to rocks referred to elsewhere in the region as the Klipkloof Granite. The distribution of Klipkloof-type Granite in the general vicinity of the Albert Silver Mine is shown on Figure 1 and on the mine area itself on Figure 2. Detailed mapping on the farm Roodepoortjie (Fig. 2) revealed the presence of two granite types; a coarse-grained, reddish, porphyritic granite (Plate 1a), which intrudes and rafts off portions of a second, fine-grained, pinkish granite containing sporadic perthitic orthoclase phenocrysts often marked by albite (Plate 1b). Geological relationships (Fig. 2; Plate 1c) indicate that the fine-grained granite is the roof zone, or possibly the chilled apical phase, into which the coarser-grained Verena phase has intruded. The ASM mineralization is, therefore, located in the upper portions of the Bushveld granite sheet, a setting very similar to many of the well-known tin deposits (e.g. Zaaiplaats Mine) elsewhere in the suite (Fig. 1).

The region of mineralization is defined on surface by at least 3 major vein systems trending approximately east-west. The north and north-east vein systems have never been mined, and the ASM deposit itself is located on the southern vein (Fig. 2). On surface the veins are distinctly gossanous and have a sub-vertical dip, comprising milky quartz, hematite, and iron-oxyhydroxide minerals.

PETROGRAPHY

Coarse-grained Porphyritic Granite (Nebo-type)

The coarse-grained porphyritic granite comprises large pink perthitic orthoclase crystals up to 2,5cm in length, together with quartz, plagioclase and biotite. Accessory minerals include zircon, fluorite, apatite, bastnaesite, monazite and occasional magnetite. Alteration of the primary minerals results in the formation of chlorite, sericite and fine aggregates of hematite-dusted clay minerals within the K-feldspar.

Fine-grained Porphyritic Granite (Klipkloof-type)

The fine-grained porphyritic granite is pinkish-grey in colour with scattered pink, perthitic orthoclase phenocrysts up to 2cm in length. Texturally the matrix varies from fine- to medium-grained and consists essentially of plagioclase, orthoclase, quartz and biotite. The

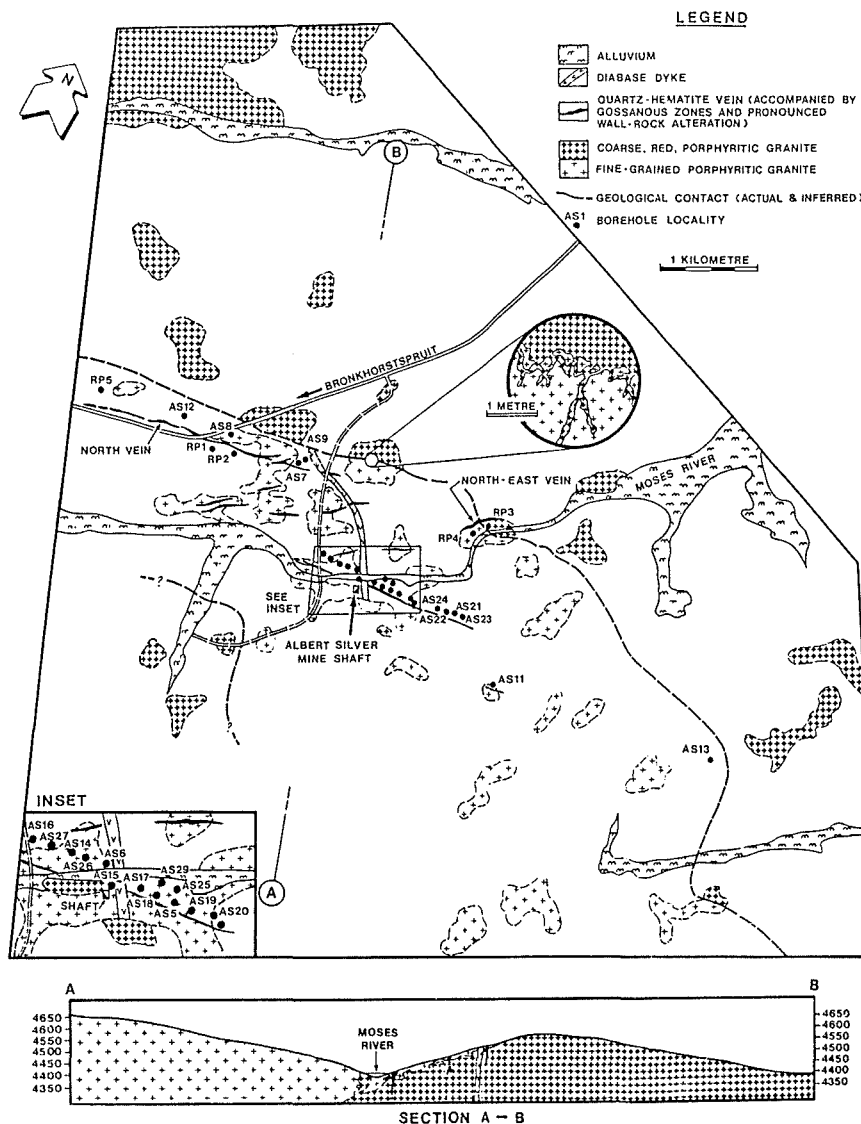


Figure 2: Outcrop map of the farm Roodepoortjie showing the distribution of the Albert Silver Mine lodes in relation to the fine- and coarse-grained porphyritic granite host rocks.

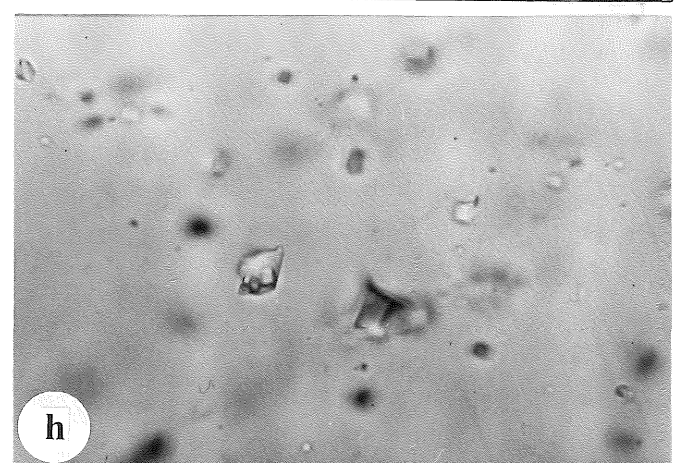
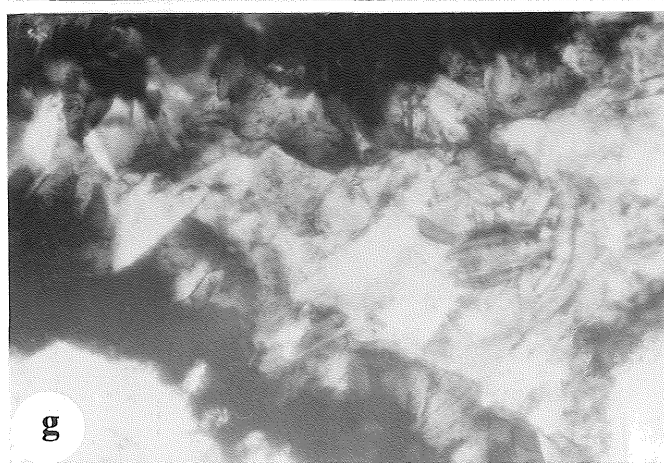
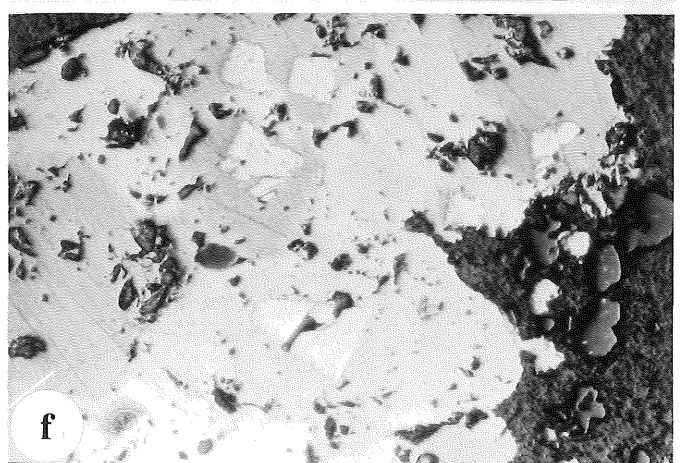
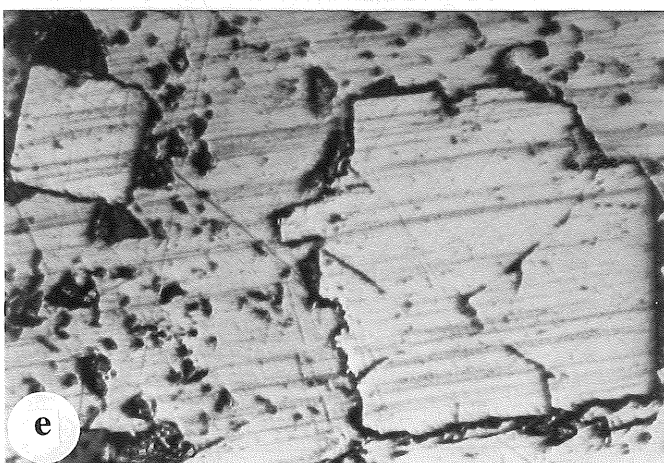
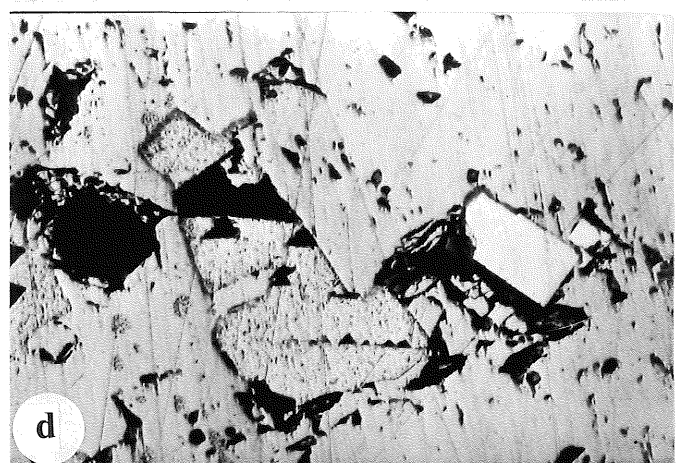
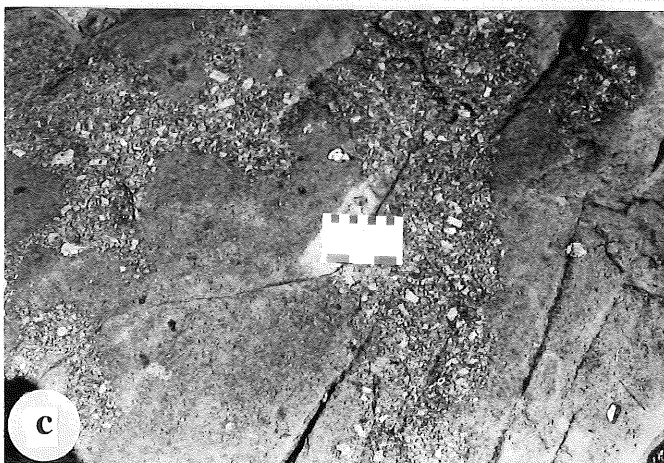
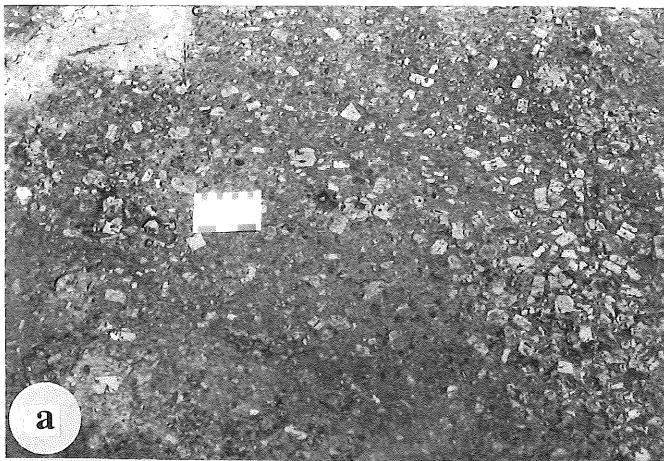
plagioclase, quartz and sphene. Accessory minerals comprise fluorite, zircon, apatite, sphene, epidote, tourmaline, bastnaesite, carbonate and magnetite-ilmenite. Alteration of the primary phases manifests itself in the form of sericitization, chloritization and the development of fine argillic alteration after feldspars.

The orthoclase phenocrysts in the fine-grained porphyritic granite often display Rapakivi-type plagioclase overgrowths (Plate 1b). Less conspicuous in the Klipkloof-type granite are white plagioclase phenocrysts, quartz phenocrysts, and three types of composite phenocrysts. These are 1) anhedral sphene rimmed by fluorite and ilmenite, 2) sericitised plagioclase enclosing apatite and zircon and surrounded by coarse-grained sphene, and 3) sericitised plagioclase with associated biotite and relatively coarse apatite, sphene, an opaque oxide, and some carbonate (possibly siderite).

PLATE 1

- a) *Coarse-grained porphyritic granite in the vicinity of Albert Silver Mine.*
- b) *Fine-grained porphyritic granite in the vicinity of Albert Silver Mine. Note isolated Rapakivi-textured feldspar megacryst.*
- c) *Contact zone between fine-grained porphyritic granite (representing the chilled apical portion of the Verena granite) and coarse-grained porphyritic granite (apophyses of which intrude up into the finer-grained phase).*
- d) *Early galena and pyrite enveloped by paragenetically later chalcopyrite. Width of field (WOF) = 0,5mm.*
- e) *Early pyrite partially corroded and replaced by chalcopyrite. WOF = 0,5mm.*
- f) *Fragmented pyrite successively enveloped by chalcopyrite and arsenopyrite. WOF = 0,5mm.*
- g) *Hematite-chlorite-fluorite vug filling representing the final stage of alteration/mineralization at Albert Silver Mine.*
- h) *Example of a high-temperature high salinity (H_2O L+V+S) fluid inclusion in quartz vein material from Albert Silver Mine. Two daughter crystals are evident. Inclusion is approximately 30 μ m in diameter.*

PLATE 1



Mineralized Veins

The three major mineralized quartz vein systems form resistant ferruginous gossan ridges on surface, but grade rapidly with depth into fresh sulphidic ore. The ore mineralogy is represented by a complex paragenetic sequence which involves early sulphide assemblages followed by a later, more oxidized assemblage comprising specularitic hematite-fluorite-chlorite-pitchblende.

The major sulphide minerals in the ore include pyrite, chalcopyrite, arsenopyrite, galena, sphalerite and argentiferous tetrahedrite. Champion (1970) also recognized the presence of minor argentite, bornite, digenite, molybdenite and a Pb-Bi-Sb sulphosalt. A readily apparent paragenetic sequence is evident among the sulphide minerals; pyrite and galena appear to have precipitated early, followed by widespread deposition of chalcopyrite (Plate 1 d and e). This phase was followed by precipitation of fahlores, principally arsenopyrite and tetrahedrite (Plate 1f). Occasionally, assayed veins yielded enhanced tin (200 - 3000ppm) and tungsten (200 - 600 ppm) contents. In one thin section cassiterite was noted along the margins of a quartz vein. These observations suggest that sulphide precipitation may have been preceded by minor deposition of Sn-W ores in the form of cassiterite and possibly wolframite.

Sulphide precipitation in the veins was followed by the paragenetically-later deposition of a more oxidized assemblage of ores comprising fluorite, chlorite, hematite (specularite) and pitchblende (Plate 1g). These assemblages generally occur as open-space fillings towards the centre of veins, or in miarolitic cavities. Pitchblende is the major uraniferous phase and occurs in association with massive hematite and as veinlets which cross-cut sulphide mineralization. Samples of massive hematitic ore taken at random from the ore-dump were occasionally found to be highly radioactive, with assay values of up to $15\text{kg}\cdot\text{ton}^{-1}$ U_3O_8 being recorded. XRF analysis of sulphidic veins occasionally yielded 170-800ppm U_3O_8 , but typically recorded values of 10-50ppm.

Late supergene alteration of the ores is characterized by the development of gossans and the precipitation of ferruginous oxyhydroxides, malachite, azurite and the rare Cu-U arsenate, metazeunerite (Champion, 1970).

Wall-rock Alteration Zones

Extensively developed zones of alteration ore developed up to 6 m away from the quartz vein system in the fine-grained porphyritic granite. Wall-rock alteration zones are distinctly greenish in colour, but become reddish and intensely silicified as the quartz-hematite vein is approached. Incipient deuteric alteration in the host granitoids is characterized by argillitization and Fe-staining of K-feldspar, sericitization of plagioclase and partial pseudomorphous replacement of biotite by chlorite. As the ore-vein is approached, primary magmatic minerals are progressively replaced by intense propylitic (chlorite + minor epidote and a CO_3 phase) and phyllic (sericite) alteration. The outer margins are generally dominated by chlorite together with lesser sericite and kaolin, while the inner alteration zones, adjacent to the veins, are intensely sericitized, with accompanying chlorite. However, as ore emplacement appears to be multi-staged, it is possible to find the superimposition of differing alteration types resulting in complex mineralogical variations and reverse zonations.

Evidence of wallrock alteration on a microscopic scale often mirrors that noted in the borehole intersections. Centred around a pitchblende stringer in the northern vein, the following mineralogical sequence was observed over a distance of 1cm; prominent pyrite mineralization adjacent to the pitchblende, enveloped by relatively coarse, clear quartz and then by a combination of fine-grained chlorite, hematite and quartz. This sequence grades into an outer sericitized and chloritized zone. Sericitization of the feldspar adjacent to the veinlet decreases after a distance of approximately 1cm away from the mineralization.

Borehole Intersections

Several phases of drilling in the period 1952-1980 were undertaken at the ASM. Some of the core has been retained and re-logged for the purpose of the present study and a typical log, represented by borehole RP2 through the north vein, is compiled in Figure 3.

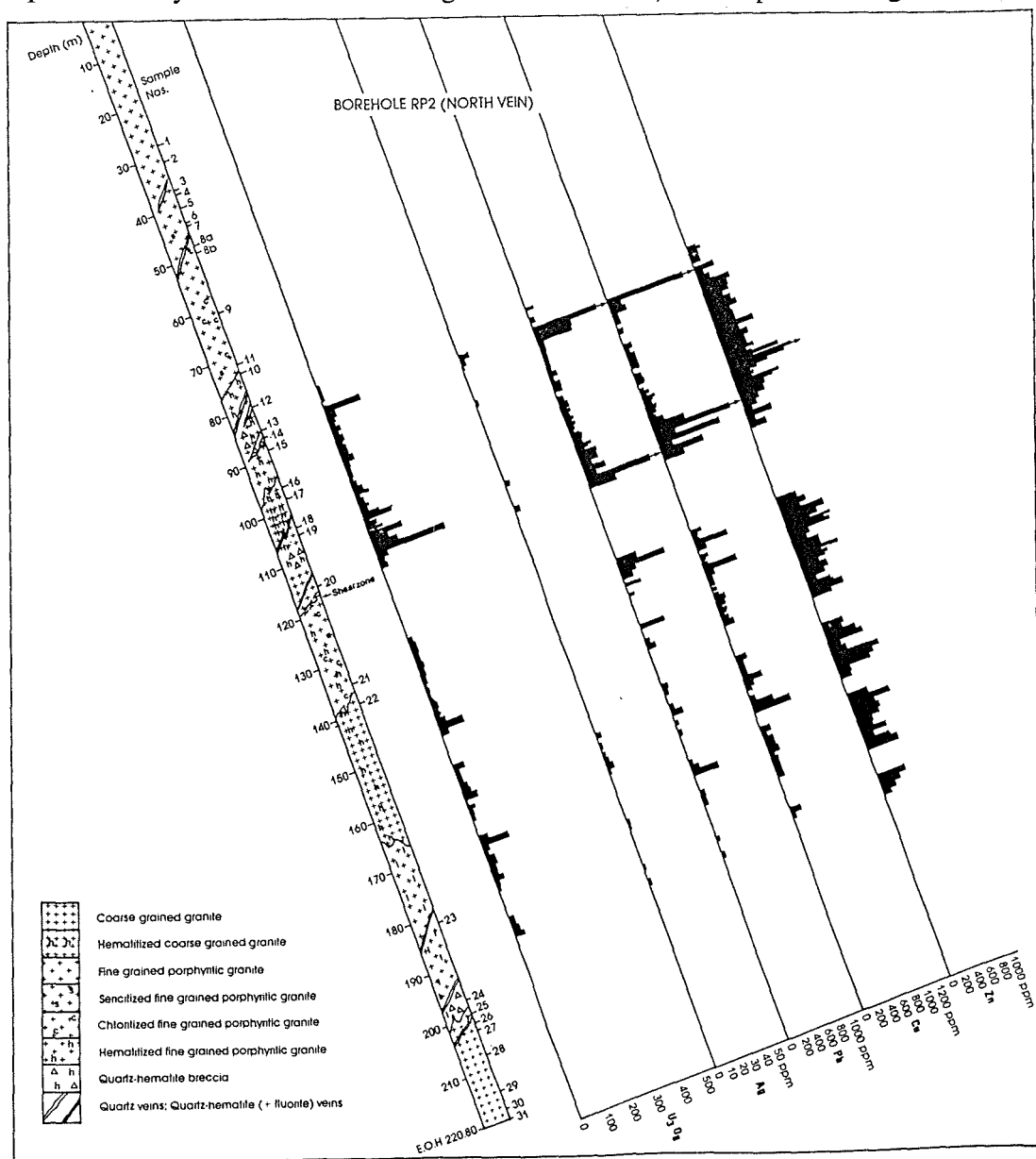


Figure 3: Simplified log of borehole RP2 showing the location of the mineralized zone and distribution of grades in relation to the fine- and coarse-grained granitic hosts.

Borehole RP2 was collared to the south of the north vein (Fig. 2) and inclined at a steep angle to intersect anticipated mineralization at circa 100m depth. The borehole passed through fine-grained porphyritic granite before intersecting sporadic quartz veins and pervasive propylitic and phyllic alteration between 50-70m below surface (Fig. 3). Intensity of veining and hematitic alteration increased markedly below 70m and a prominent zone of Cu-Pb-Zn-Ag-U mineralization was intersected between 85-120m depth. Vein orientation is subvertical, although occasional zones of brecciation/vein stockworking occur. Between 100-200m depth the core revealed a fairly complex mixed zone comprising both fine-grained and coarse-grained porphyritic granite, suggesting the presence of a contact zone similar to that documented on surface (Fig. 2). Sporadic mineralization occurs throughout this contact zone (Fig. 3), but then diminishes dramatically below approximately 190m depth. Below 200m only coarse-grained porphyritic granite is present, and this rock is typified by only incipient deuteric alteration, few veins and no mineralization. It is apparent from this, and other boreholes logged that while mineralization is, at first glance, apparently related to sub-vertical veins and their associated wall-rock alteration, on a broader scale it is distributed along a sub-horizontal zone represented by the contact between the fine-grained granite "roof" and underlying coarser-grained granite. Consequently, at ASM veins do not penetrate to great depths within the granite, but appear to be localized in a *stratiform* zone, only a few tens of metres thick, in the apical portions of the granite body. This trait has important implications for the exploration of other polymetallic deposit types in the Bushveld.

GEOCHEMICAL CHARACTERISTICS OF HOST GRANITOIDS

A total of 52 samples from the ASM, collected from surface or borehole intersections, have been analysed for major and selected trace elements (by XRF spectrometry) and for rare earth elements (by instrumental neutron activation analysis). A representative subset of the data is presented in Table 1; the complete data set is available from the senior author on request.

Both granitoid types in the vicinity of the Albert Silver Mine are leucocratic, low-Ca granites (*sensu stricto*) which are marginally peraluminous to metaluminous. They are classified as A-type granites, a feature demonstrated originally for the Bushveld granites by Kleemann and Twist (1989), who pointed to their high Ga/Al₂O₃ ratios and compatibility on a CaO - Al₂O₃ - (Na₂O + K₂O) ternary plot with the established field of A-type granitoids (Fig. 4). A-type granites, derived from anhydrous lower crust, are typically emplaced in anorogenic environments, are alkaline in composition with high Ga/Al₂O₃, Fe/Mg, SiO₂, Zr, F, low Ca and Sr, and a Sn-Mo-Bi-Nb-W-Ta-F metallogenic association (Collins et al., 1982). Confirmation of the A-type character of the Albert Silver Mine granitoids is presented on the SiO₂ versus Nb, Y, Zr plots of Figure 5. Both altered and unaltered variants of the ASM granitoids fall within the field of A-type granitoids defined by Collins et al. (1982) and overlap with the fields of two A-type suites in Australia.

Parts of the Bushveld granite are highly differentiated, and are characterized by high Rb/Sr, Rb/Ba and low K/Rb ratios. Data plotted on a Rb-Sr-Ba ternary diagram (Fig. 6) confirm that the ASM granitoids are also highly differentiated. It is also evident in Figure 6 that granitoids associated with mineralization show extreme depletions in Sr and Ba (Table 1) and accordingly plot towards the Rb apex of the diagram, a feature typical of albitized and greisenized granites.

TABLE 1: CHEMICAL ANALYSIS OF SELECTED SAMPLES FROM THE ALBERT SILVER MINE

	1	2	3	4	5	6	7
	A9	RP2-28	A10	AS13-2	RP1-5	RP1-19	RP1-20
SiO ₂	77,10	73,90	72,00	73,30	73,40	65,60	77,40
TiO ₂	0,19	0,21	0,33	0,22	0,32	0,30	0,30
Al ₂ O ₃	11,50	12,50	13,90	13,40	13,10	9,71	13,10
Fe ₂ O ₃	1,86	2,16	3,68	2,22	2,96	18,80	1,61
MnO	0,02	0,07	0,07	0,08	0,02	0,77	0,03
MgO	0,20	0,45	0,70	0,70	0,57	0,83	0,34
CaO	0,45	0,85	0,71	0,20	0,13	0,06	0,11
Na ₂ O	3,70	3,60	4,80	3,60	3,20	0,01	0,20
K ₂ O	4,48	4,73	4,30	4,97	4,93	0,40	3,79
P ₂ O ₅	0,01	0,04	0,06	0,06	0,07	0,05	0,07
L.O.I.	0,61	1,28	0,92	0,93	1,08	2,79	2,35
Totals	100,13	99,80	101,15	99,68	99,82	99,38	99,44
Ba	270	405	240	501	562	48	40
Rb	280	292	287	355	368	45	322
Sr	-	32	-	50	12	1	2
Y	-	69	-	77	75	121	95
Zr	-	224	-	253	323	290	329
Nb	-	32	-	28	30	31	32
U	18	17	1	10	17	16	28
Th	47	41	31	7	20	10	7
La	-	88	102	78	86	75	56
Ce	143	179	169	146	141	117	102
Nd	52	53	51	47	81	54	47
Sm	-	11	12	11	11	11	10
Eu	0,7	0,8	1,1	1,2	1,2	1,8	1,2
Tb	1,5	1,5	1,7	1,7	1,7	2,7	1,8
Yb	7,1	6,7	7,1	7,0	12,2	12,2	8,4
Lu	1,3	0,8	1,2	1,2	1,2	1,2	0,9

Columns 1-2: Coarse grained porphyritic granite (Nebo-type)

3-5: Fine grained porphyritic granite (Klipkloof-type)

6-7: Altered granite adjacent to mineralized veins

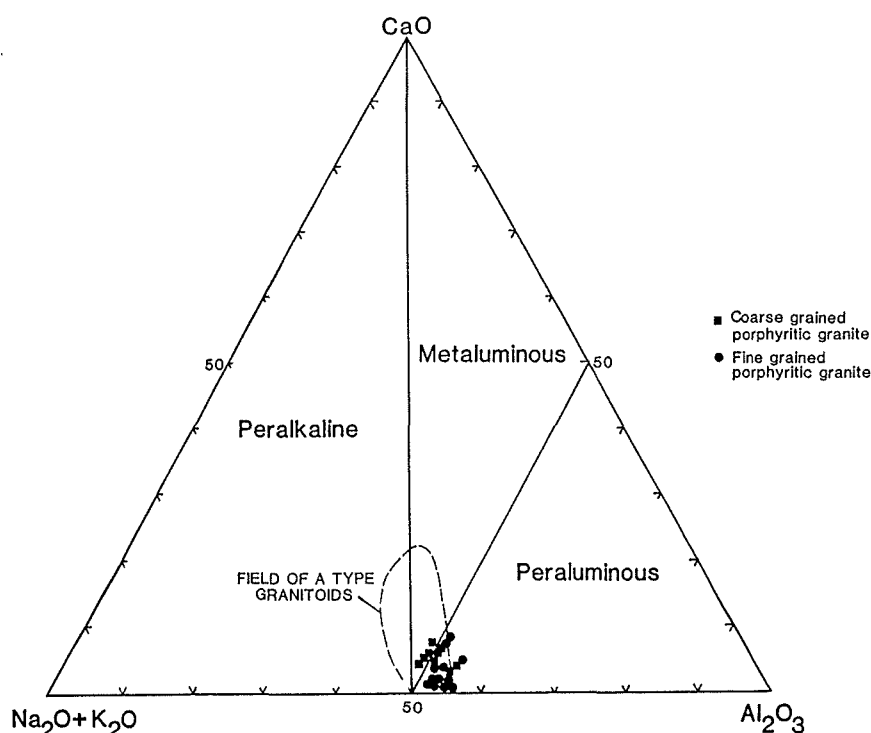


Figure 4: Composition of Albert Silver Mine granitoids in terms of $\text{CaO}-\text{Na}_2\text{O}+\text{K}_2\text{O}-\text{Al}_2\text{O}_3$ ternary diagram.

The various phases and textural sub-types of the Bushveld granites can be genetically related through a process of Rayleigh fractionation and in situ crystal fractionation (McCarthy and Hasty, 1976; Groves and McCarthy, 1978; Walraven et al., 1985). A plot of an incompatible trace element (e.g. Rb) versus a compatible trace element (e.g. Ba) for unaltered Bushveld granites (Fig. 7a) reveals a trend that is characteristic of a liquid-line-of-descent controlled largely by feldspar fractionation. In Figure 7a unaltered granitoids from ASM reflect the strongly differentiated aspect of this suite and plot in the field of the Bobbejaankop Granite, which is the host to tin mineralization at the Zaaipplaats Mine (Fig. 1). Altered granitoids from ASM show extreme depletion of Ba, a feature related to hydrothermal alteration of feldspars and mobilization of Ba during the mineralization process.

In Figure 7b, where unaltered granites from the ASM area are plotted, it is pertinent to note that the fine-grained porphyritic granite is marginally more enriched in Rb than the coarse-grained porphyritic granite. This relationship can be modelled using Rayleigh fractionation curves for an initial magma composition at C_0 and suggests that the coarse-grained porphyritic granite represents a cumulate-like product of a fairly advanced degree of fractionation, while the fine-grained porphyritic granite has a trace element signature that approximates the original liquid composition. This model confirms the earlier suggestion that the fine-grained variant is the rapidly cooled roof of the Verena Porphyritic Granite which is underlain, and intruded into, by a more highly fractionated coarser-grained equivalent of the same magma chamber.

In the plot of U versus U/Th in Figure 8 some interesting features emerge regarding the radio element distribution in the host rocks of the ASM. In this type of plot, lines radiating from the origin represent equal Th contents, while increasing U/Th ratios reflect

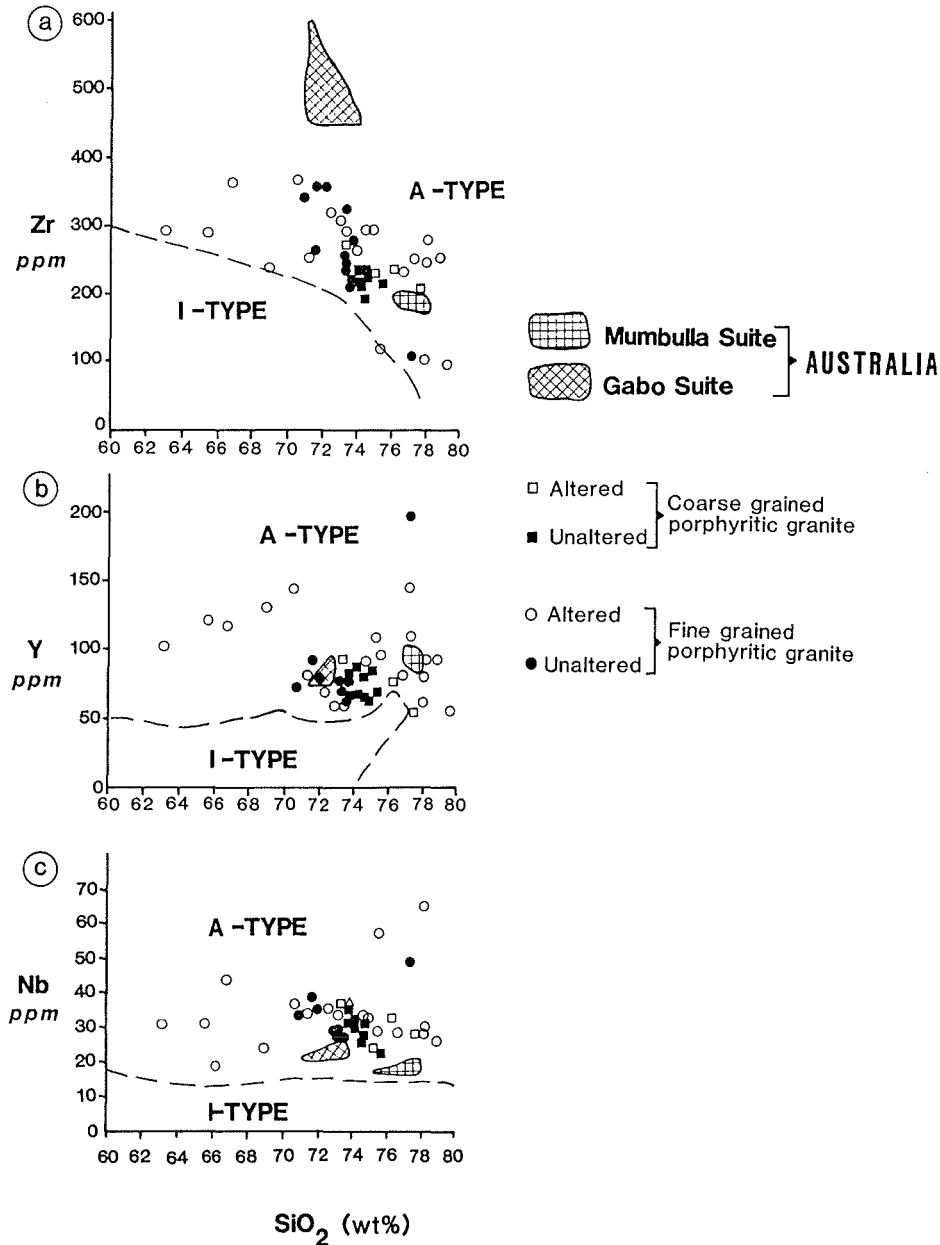


Figure 5: Plots of (a) $\text{Zr} \text{ v } \text{SiO}_2$ (b) $\text{Y} \text{ v } \text{SiO}_2$ and (c) $\text{Nb} \text{ v } \text{SiO}_2$ showing the A-type character of the Albert Silver Mine granitoids. Mumbulla and Gabo suite data after Collins et al. (1982).

the degree to which U or Th have been decoupled (with regard to primary or magmatic ratios where $\text{U/Th} = 0.25$). Most of the samples of the coarse-grained porphyritic granite fall on the $\text{Th} = 36 \text{ ppm}$ curve whereas most of the fine-grained porphyritic granites fall on the $\text{Th} = 22 \text{ ppm}$ curve. This is consistent with the notion that the coarse-grained phase is more fractionated than the fine-grained phase. By contrast, most of the samples from the altered wall-rock to the ore-veins fall on low Th curves and have high U/Th ratios in the range 1-3. This suggests that uranium has been strongly decoupled from, and enriched relative to, Th. The unaltered host rocks have U/Th ratios which are typically < 1 , values which, although enriched relative to the clarkite, reflect fairly typical magmatic properties. The markedly higher U/Th ratios in altered and mineralized wall-rock, compared to the typically magmatic U/Th ratios in unaltered granites, clearly indicates that the alteration process itself has been

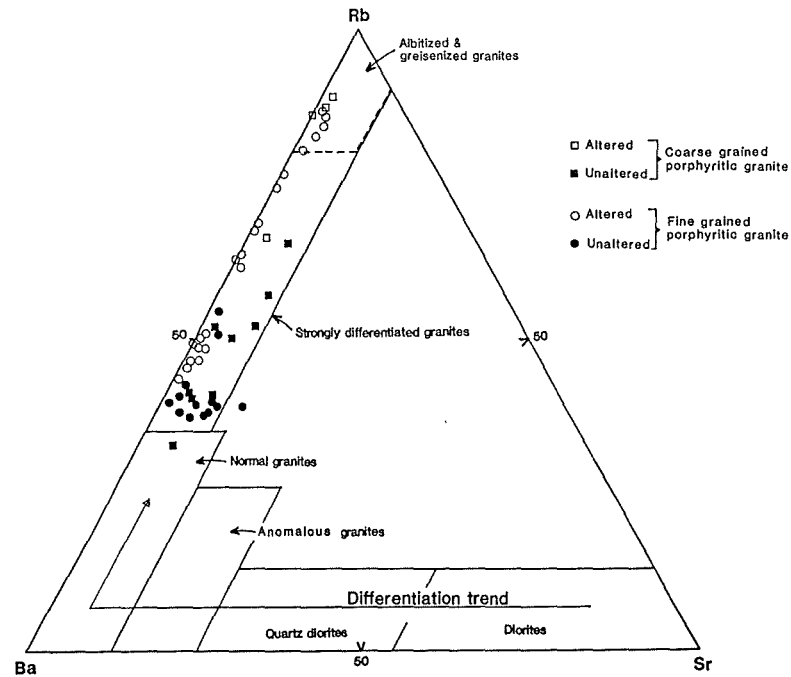


Figure 6: Ternary Rb-Sr-Ba diagram showing the characteristics of altered and unaltered coarse- and fine-grained porphyritic granites from Albert Silver Mine.

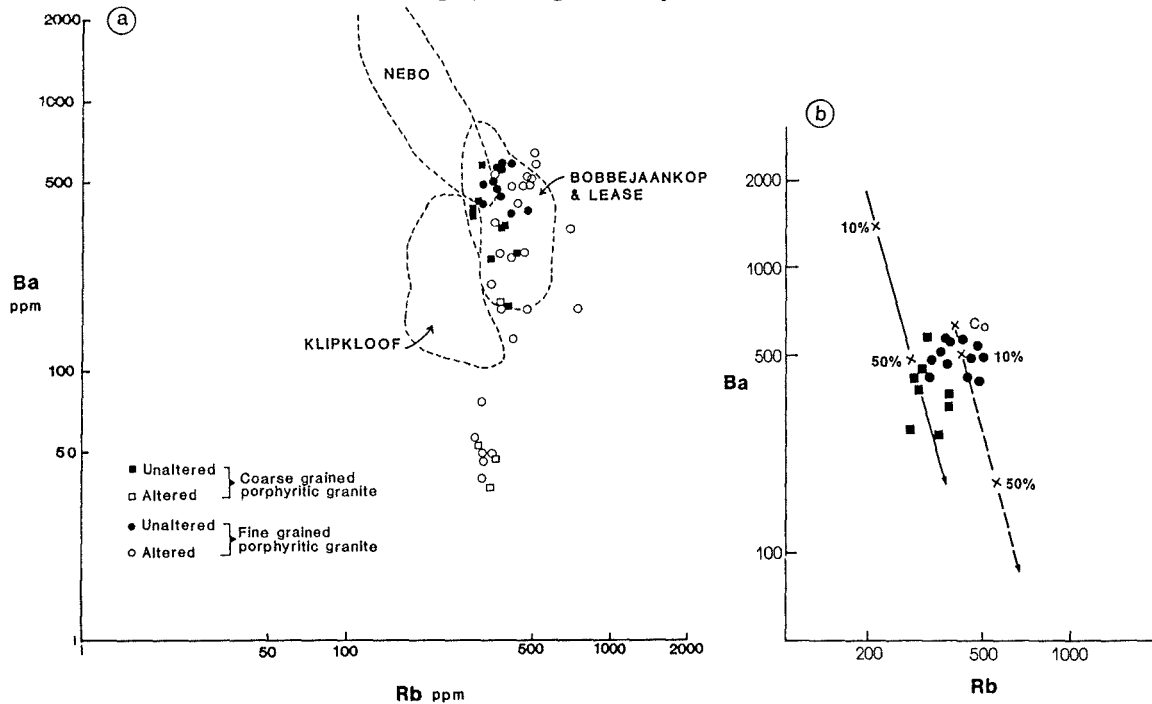


Figure 7 (a) Rb v Ba plot for Albert Silver Mine granitoids in relation to the fields of other Bushveld Complex granitoids (after Walraven et al., 1985); (b) Rb v Ba plot for unaltered Albert Silver Mine granitoids in relation to model Rayleigh Fractionation curves (C_0 - initial liquid composition; 10%, 50% - degree of crystallization; solid line - concentrations in the solid phases; dashed line - concentrations in the residual liquid). According to this model the coarse-grained porphyritic granite resembles a cumulus assemblage while the fine-grained porphyritic granite resembles a (chilled?) liquid-like composition.

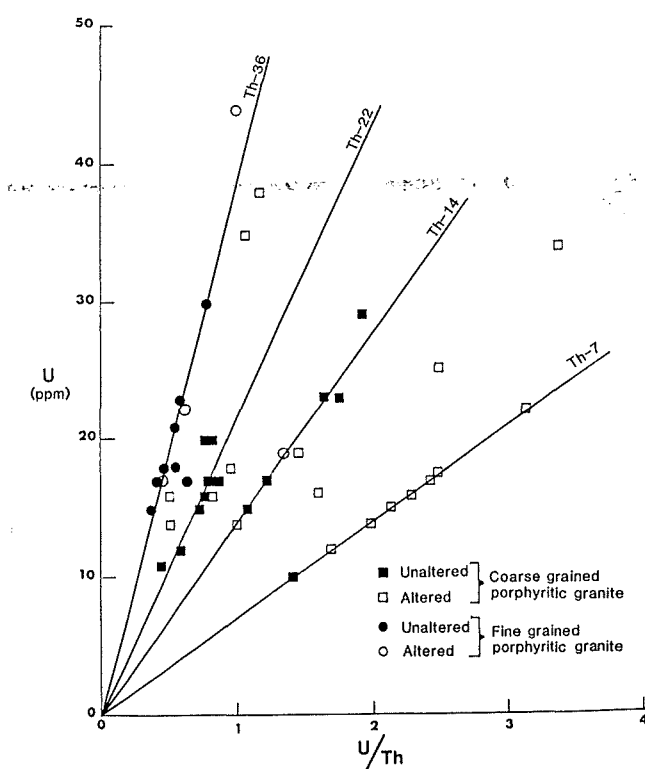


Figure 8: Plot of U v U/Th for Albert Silver Mine granitoids. Altered granitoids are often characterized by high U/Th ratios indicating that the two radioelements have been decoupled with U strongly concentrated in the mineralized portions of the system.

responsible for mobilization of uranium. This strongly suggests that concentration of uranium into the hematite-pitchblende-fluorite-chlorite veins is related to the evolving endogranitic hydrothermal system, and not to later processes.

REE traces for altered ASM granitoids display enriched LREE, marked negative Eu anomalies, and flat HREE distribution patterns (Fig. 9a). The coarse-grained porphyritic granites have the largest negative Eu anomaly, and this consistently distinguishes the latter from the (less differentiated) fine-grained porphyritic granites. The REE distribution in altered wall-rock samples is illustrated in Figure 9b, where it is clear that the patterns between altered and unaltered rock types are very similar, although minor differences do occur. Wall-rock alteration adjacent to the mineralized quartz veins is zoned and comprises an inner sericitic zone which grades outwards into propylitic alteration. Although both propylitic and phyllic zones of alteration are slightly depleted in LREE and enriched in HREE compared to unaltered fine-grained porphyritic granite, the degree of REE mobilization is very slight even though other elements, such as Na, Ca, Ba and Sr, have been markedly depleted (Table 1). It is apparent from this observation that the fluids involved in mineralization and wall-rock alteration did not favour the complexing of REE either as a group, or selectively. The coherent REE patterns in the propylitic and sericitic wall-rock zones adjacent to the mineralized veins therefore reflect either relatively low fluid/rock ratios, or the existence of a hydrothermal fluid deficient in REE-complexing ligands.

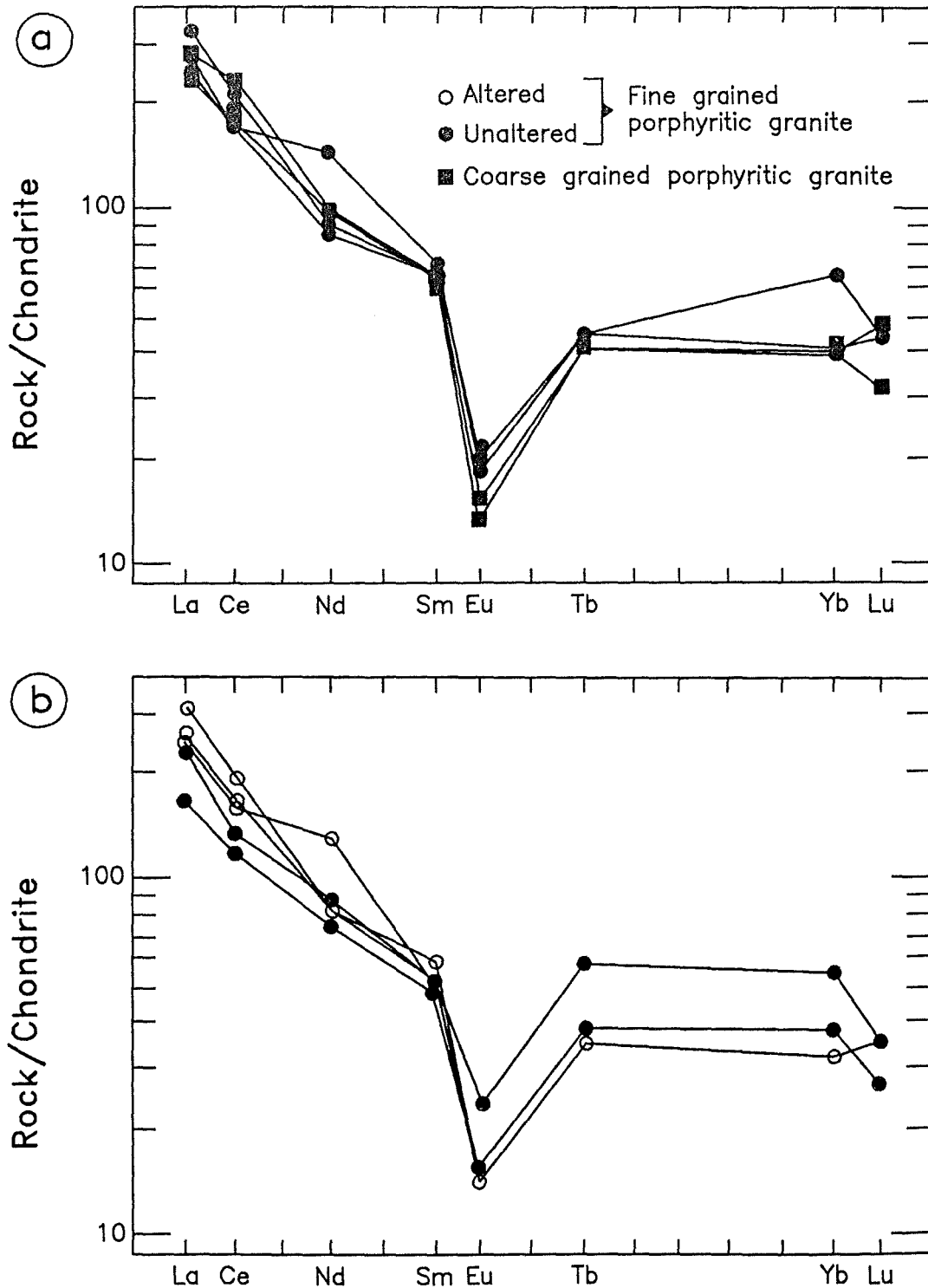


Figure 9: Chondrite normalized rare earth element plots for (a) Albert Silver Mine granitoids and (b) comparing altered and unaltered fine-grained porphyritic granite.

Propylitic and phyllic alteration zones associated with porphyry Cu-Mo systems also exhibit relatively pristine REE patterns, with only slight leaching of LREE (Taylor and Fryer, 1983), as in the present case. Likewise, HREE are progressively less soluble when associated with aqueous brines depleted in CO_2 , a feature consistent with the present study which indicates moderately saline brine and an absence of CO_2 (see later).

ORE FLUID CHARACTERISTICS

Attempts to characterize the nature of the ASM ore-fluids have been made with the use of fluid inclusion microthermometry, together with chlorite analysis and the application of the Al(IV) occupancy in chlorite geothermometer of Cathelineau and Neiva (1985).

Preliminary fluid inclusion microthermometry was undertaken on quartz from two samples; the one from relatively unaltered coarse-grained porphyritic granite (RP2-28), and the other (RP2-11a), from highly altered, quartz-veined, fine-grained porphyritic granite in the main mineralized zone (Fig. 3). Fluid inclusions in both samples are dominated by two phase aqueous inclusions (H_2O L+V) with approximately 10% three phase inclusions (H_2O L+V+S) comprising mainly one, and sometimes two, daughter crystals (Plate 1h). CO_2 was not detected as a separate phase in any inclusion although a low molar proportion of CO_2 in the aqueous inclusion is suggested by the occasional presence of clathration. Phase changes observed in freezing runs indicate fairly complex, multi-component fluid systems and at least two fluid populations. In Figure 10 (a and b) fluids are seen to exhibit eutectic melting at around -50°C , possibly suggesting the presence of CaCl_2 in addition to NaCl (i.e. eutectic melting in the system $\text{H}_2\text{O} - \text{CaCl}_2 - \text{NaCl}$ is -52°C). A pronounced final melting peak is evident at around -20°C (equivalent to 22 wt.% eNaCl) while a smaller proportion of inclusions melted completely at between -5 and 0°C , indicating a less saline fluid population (<8 wt.% eNaCl). Fluid inclusions with daughter crystals were heated to 500°C without complete dissolution of the solid phase taking place; homogenization or decrepitation invariably occurred prior to daughter crystal dissolution. Two fluid populations are also suggested during the heating cycle, with one T_h peak occurring at $150 \pm 30^\circ\text{C}$, and another high kurtosis population defined between 260 - 460°C (mean = 350°C) (Fig. 10c). It is apparent in the latter diagram that the unaltered coarse-grained porphyritic granite (RP2-28) is dominated by low T_h fluids at around 150°C , (density = $0,97\text{g.cm}^{-3}$; calculated using the equation of state for H_2O -NaCl after Brown and Lamb, 1989) while the mineralized and highly altered sample (RP2-11a) has an apparently higher proportion of high T_h fluids (with densities of around $0,89\text{g.cm}^{-3}$). The presence of two apparently distinct fluid populations cannot at this stage unequivocally be related to the ore paragenesis since fluid inclusion petrography did not allow this distinction to be made and no microthermometric measurements were undertaken on, for example, the paragenetically late fluorite. It is nevertheless tempting to suggest that the saline, high-temperature fluid was linked to the early sulphide paragenesis at ASM while the less saline, lower-temperature fluid was associated with the later hematite-pitchblende-fluorite-chlorite mineralization. Further work on the fluid inclusion characteristics of these ores is currently being undertaken.

Chlorite compositions determined on an electron microprobe (Table 2) were determined for a number of ore samples, including chlorite pseudomorphs after biotite (in coarse-grained porphyritic granite RP2-30) and hydrothermal chlorite in the propylitic wall-rock alteration zone (RP1-18), as well as chlorite in quartz-sulphide veins (AS25-10c) and in the paragenetically late hematite-pitchblende-fluorite-chlorite ore (AS15-3; Table 2). All the chlorites analysed are markedly ferroan in composition with a low number of Si^{4+} cations in the structural formula (calculated with reference to 14 oxygens) and $\text{Fe}^{2+}/\text{R}^{2+}$ approaching unity (Table 2). Using Foster's (1962) classification scheme all chlorites from the ore body are distinctly thuringitic in composition, while the chlorite which replaces biotite in the coarse-grained porphyritic granite is ripidolite. Extremely ferroan chlorites such as those

TABLE 2: CHLORITE ANALYSES OF SELECTED SAMPLES FROM THE ALBERT SILVER MINE

Sample	AS25-10c	RP1-18	RP2-30	AS15-3
No. of analyses	4	10	5	2
SiO ₂	22,49	24,14	23,27	23,65
Al ₂ O ₃	18,98	18,93	15,11	20,16
FeO	37,31	39,56	24,36	40,00
MnO	1,55	1,39	1,31	1,50
MgO	0,97	1,70	5,75	1,55
Na ₂ O	0,04	0,03	0,10	0,09
K ₂ O	0,03	0,42	0,05	0,01
TiO ₂	0,02	0,02	0,84	0,00
Cr ₂ O ₃	0,01	0,02	0,01	0,01
CaO	0,06	0,01	0,09	0,10
Cl	0,06	0,06	0,04	0,04
Totals	81,52	86,28	70,93	87,11
Si ⁴⁺	2,13	2,28	2,20	2,26
Fe ²⁺	2,95	3,12	1,92	3,16
Mg ²⁺	0,14	0,24	0,81	0,22
R ²⁺	3,09	3,36	2,73	3,38
Fe ²⁺ /R ²⁺	0,95	0,93	0,70	0,93
Al(IV)	1,87	1,72	1,80	1,74
Al(IV)corr.	2,53	2,37	2,29	2,39
Al(VI)	2,36	2,49	1,56	2,75
T°C	286	269	260	271

NOTES: (i) Analyses carried out on a CAMECA electron microprobe at the Department of Geology, University of the Orange Free State

(ii) Structural formulae calculated with respect to 14 oxygens (½ cell)

(iii) Al(IV)corr. - Tetrahedral Al site occupancy corrected for high Fe contents using factors of Kranidiotis and Maclean (1987)

(iv) T°C - temperatures of chlorite formation after Cathelineau and Neiva (1985).

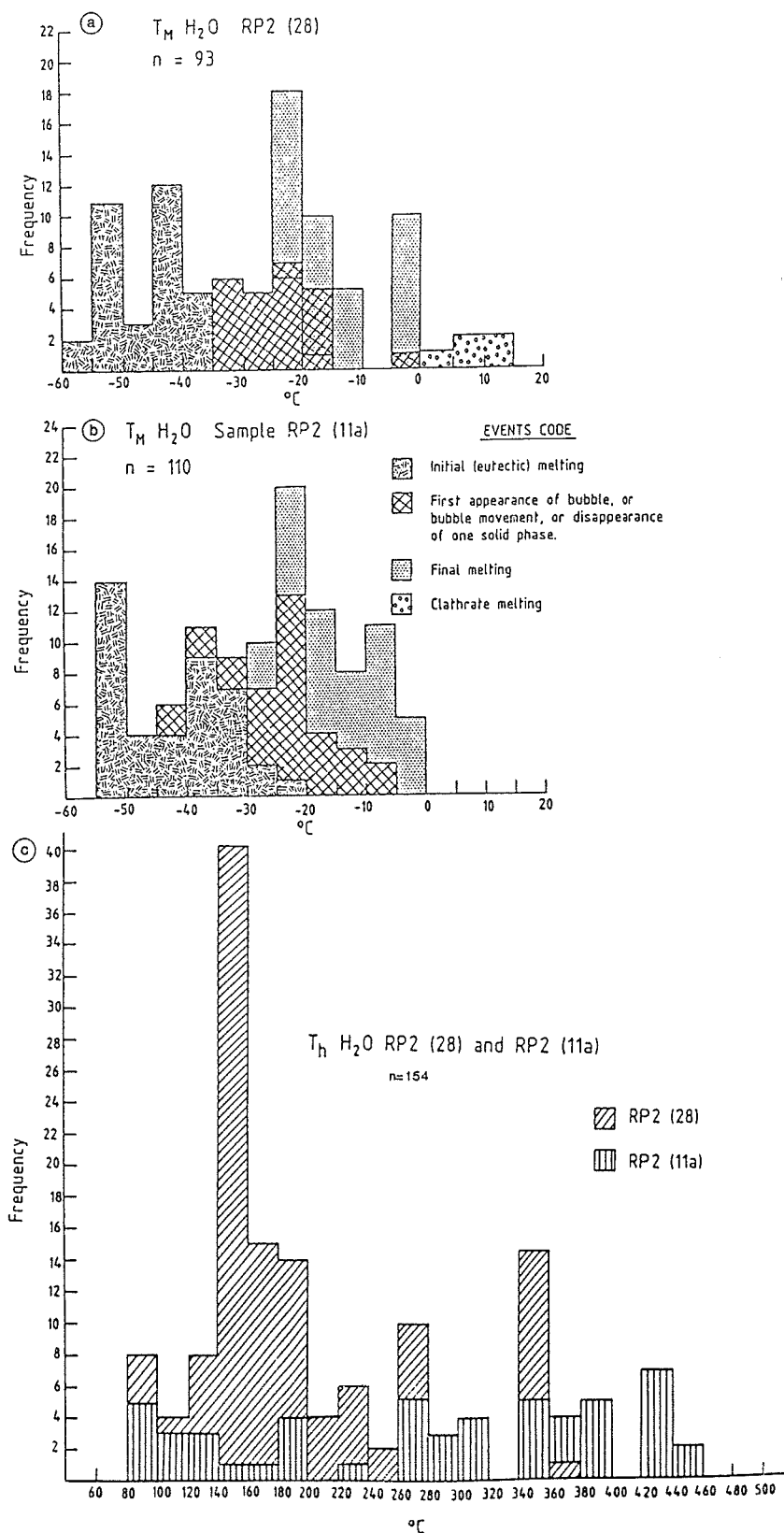


Figure 10: Summary of fluid inclusion microthermometry from the Albert Silver Mine; (a) and (b) - low temperature phase changes for samples RP2-28 and RP2-11a; (c) homogenization temperatures (H₂O L → V) for the same samples.

from the ASM ore-zone usually suggest a high proportion of Fe_2O_3 (4-12%; Foster, 1962), or Fe^{3+} , which replaces Al^{3+} in the chlorite lattice. This is supported, in the case of the ASM ore-body chlorites, by the presence of a substantial surplus of octohedral, compared to tetrahedral, alumina occupancy (Table 2) which results in the sort of charge imbalances typically redressed by ferric iron substitution (Foster, 1962). The presence of a substantial ferric iron component in the chlorite lattice indicates a high $f\text{O}_2$ fluid (hematite-magnetite buffer) in equilibrium with the alteration assemblage.

Chlorite compositions have also been processed in terms of the Al(IV) geothermometer of Cathelineau and Neiva (1985), with the Al(IV) site occupancy corrected for high Fe/Fe+Mg ratios using the factors of Kranidiotis and Maclean (1987). Temperatures of formation for all the chlorites analysed range between 260-290°C and appear to be independent of the type of chlorite and the major element variations observed.

RADIOGENIC ISOTOPE CHARACTERISTICS

Several samples of unaltered borehole material were sampled specifically for Rb-Sr and Pb-Pb whole rock and Pb-Pb mineral isotope analysis in order to gain insight into the nature of the mineralization at ASM. The data presented below should be considered in the light of a new and precise U-Pb zircon age of 2054.4 ± 1.8 Ma for the main phase of the Bushveld granite (Walraven and Hattingh, 1993).

The results of the Rb-Sr isotope whole rock analyses of Nebo Granite are listed in Table 3 and illustrated in Figure 11a. Considerable scatter is present in the data for the four samples analysed suggesting that open-system behaviour occurred in the granite. A reference isochron with an age of 2050 Ma and an initial $^{87}\text{Sr}/^{86}\text{Sr}$ ratio (I_0) of 0.72 shows sample RP2-30 (relatively unaltered coarse-grained porphyritic granite) to plot on the reference isochron while the other samples (variably altered and mineralized coarse-and fine-grained porphyritic granite) plot off the line. Open-system isotopic behaviour is common among granites of the Bushveld Complex (Walraven, 1981; Walraven et al., 1985; 1990) which commonly yield dates up to 250 Ma younger than the true age of emplacement (Walraven, 1987). The isotope systematics observed in the present study differ from others where isotope ratios usually result in straight-line relationships among the data points and isochrons with demonstrably low ages. Samples in the present study (all collected from in and around the zone of mineralization) are characterized by variable degrees of alteration (and fluid-rock interaction) which possibly accounts for the incoherent isotope ratios observed in the ASM samples.

Whole-rock Pb-Pb data for the same samples are listed in Table 3 and illustrated in Figure 11b. These data show that the whole-rock Pb systems have also been affected by open-system behaviour since the data are scattered and show little or no bearing to the 2050 Ma reference isochron. Sample RP2-30, consisting of unaltered coarse porphyritic granite, plots, like the Rb-Sr data, reasonably close to the 2050 Ma reference isochron. The three altered samples are, by contrast, colinear and define an age of around 500 Ma. This 'age' does not have any geological relevance and the colinearity of points is likely to be coincidental. Also included on Figure 11b are the results of Pb isotopic analyses of galena derived from a quartz-sulphide vein in a phyllic alteration zone (RP2-8a and b) and from a propylitic altered zone comprising late, vuggy fluorite, galena and carbonate (RP1-24).

TABLE 3: RB-SR AND PB-PB ISOTOPIC ANALYSES OF SELECTED SAMPLES FROM THE ALBERT SILVER MINE

	Rb(ppm)	Sr(ppm)	$^{87}\text{Rb}/^{86}\text{Sr}$	$^{87}\text{Sr}/^{86}\text{Sr}$	$^{206}\text{Pb}/^{204}\text{Pb}$	$^{207}\text{Pb}/^{204}\text{Pb}$	$^{208}\text{Pb}/^{204}\text{Pb}$
WHOLE ROCK							
AS9-1	257.5	57.84	13.09	1.068013	19.306	15.460	37.593
				$\pm .000007$	$\pm .001$	$\pm .001$	$\pm .003$
AS16-2	304.4	73.87	12.06	1.022876	21.320	15.597	35.893
				$\pm .000011$	$\pm .001$	$\pm .001$	$\pm .003$
RP1-10b	281.4	41.80	19.96	1.159875	23.267	15.670	39.886
				$\pm .000010$	$\pm .001$	$\pm .001$	$\pm .003$
RP2-30	279.3	47.62	17.47	1.210519	26.220	16.128	43.750
				$\pm .000089$	$\pm .002$	$\pm .002$	$\pm .004$
GALENA							
RP1-24					17.208	15.269	35.863
					$\pm .002$	$\pm .001$	$\pm .003$
RP2-8a					15.006	14.953	34.394
					$\pm .002$	$\pm .001$	$\pm .004$
RP2-8b					15.172	14.973	34.554
					$\pm .003$	$\pm .002$	$\pm .005$

- For sample descriptions see text

- Isotope analyses carried out on a MAT261 mass spectrometer, Isotope Section, Geological Survey of South Africa

- For analytical details see Walraven et al., 1990.

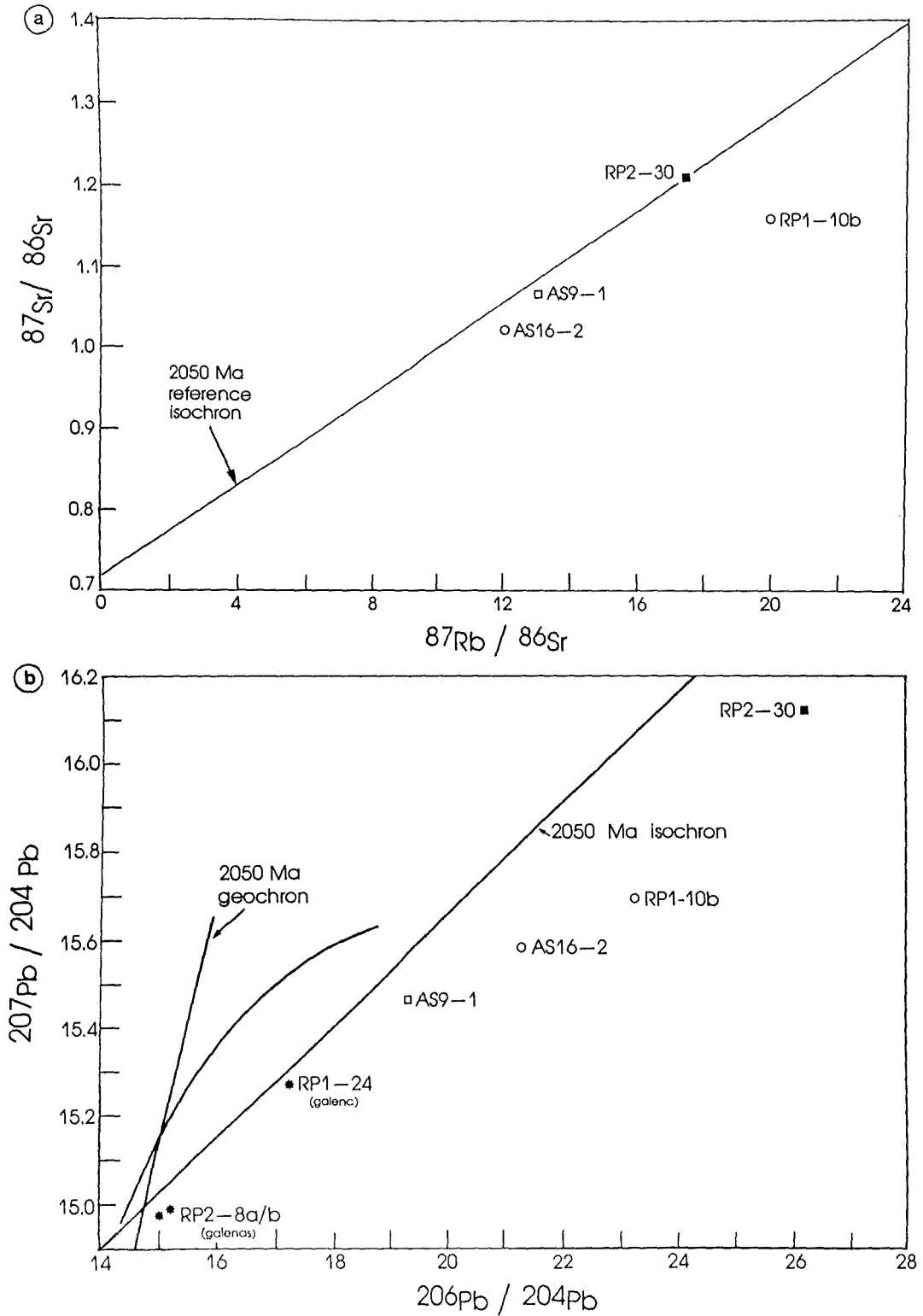


Figure 11: (a) $^{87}\text{Sr}/^{86}\text{Sr}$ vs $^{87}\text{Rb}/^{86}\text{Sr}$ plot for unaltered (RP2-30) and altered/mineralized (AS16-2, AS9-1 and RP1-10b) granitoid samples from Albert Silver Mine; (b) $^{207}\text{Pb}/^{204}\text{Pb}$ vs $^{206}\text{Pb}/^{204}\text{Pb}$ plot for the same whole rock samples as well as three galena separates from the Albert Silver Mine ore-zone.

Samples RP2-8a and RP2-8b have very similar, relatively unradiogenic, isotopic compositions (Fig. 11b), while RP1-24 is different and distinctly more radiogenic. The less radiogenic samples have model ages of 1672 and 1574 Ma ($\mu = 8.06$ and 8.04 respectively), which is considerably younger than the age of the host granite. The more radiogenic sample has an even lower model age of circa 400 Ma ($\mu = 8.51$).

Open system behaviour and isotopic disturbance of the Bushveld granites, especially in the Rb-Sr system, has yielded isochrons that are younger than the emplacement age, a feature that is attributed to selective removal of radiogenic Sr primarily from K-feldspar by late-stage magmatic or hydrothermal fluids (Walraven, 1981; Walraven et al., 1990). Significant Pb-loss, especially in high-U zircons, is also reported from Bushveld granites (Walraven, 1987). In the case of the ASM, whole rock Rb-Sr and Pb-Pb data are too scattered to define isochrons and point to severe, but variable, degrees of isotopic disturbance in and around the deposit. Such a scatter is consistent with a mineralizing system characterized by a complex paragenetic sequence (probably active over a lengthy period of time) and highly variable fluid/rock ratios over short distances adjacent to vein systems. Studies of Rb-Sr isotope systematics adjacent to zones of tin mineralization also reveal open-system behaviour where the degree of ^{87}Sr loss is proportional to the severity of alteration (Walraven et al., 1990).

The discrepancy in galena Pb isotopic data can be explained either by the existence of two phases of mineralization at different times, or multiple sources of Pb having different isotopic compositions. At the time of emplacement of the Bushveld Complex, Pb in the granite and its roof rocks (granophyre and rhyolite) was insufficiently evolved to account for the relatively radiogenic Pb isotopic compositions observed. Mineralization at this time would therefore require older, more evolved, sources of Pb. If, however, the galena formed at a later stage, about 400 Ma after granite emplacement (as suggested by the model ages of the RP2 samples), the Pb in the upper, highly differentiated portion of the granite sheet could have been sufficiently evolved to have the isotopic composition observed in the ASM galenas. Models in which the Pb was entirely derived from the Bushveld granite itself, or mixed in various proportions with more evolved Pb, would be consistent with the notion of a long-lived mineralization event, lasting for at least 400 Ma after granite emplacement.

Alternatively, the data could be interpreted to reflect the ages of two discrete mineralization events, the older age (1600-1700 Ma) corresponding to the age of the late-stage processes that widely affected the Bushveld acid rocks, while the younger age (400 Ma) would imply a later unrelated event. This option is considered unlikely, however, as all the available geological evidence points to a genetically related paragenetic sequence, and there is little or no evidence for a discrete younger event.

DISCUSSION

Styles of Polymetallic Mineralization in the Bushveld Granites

Certain portions of the Lebowa Granite Suite are particularly well-endowed with innumerable small-to medium-scale polymetallic deposits. These deposits collectively identify the Bushveld granite as a highly prospective metallotect which has probably not received the exploration attention that it is due. A wide variety of metals, of which Sn-W-

Pb-Zn-Bi-Co-Mo-Ag-Au-F-U-REE are the most important, have been concentrated within or adjacent to the various phases of the Bushveld granites by processes related to the crystallization and subsequent fluid evolution of this suite. The first attempt to genetically relate the wide variety of ore deposit types in the Bushveld granites was made by Crocker (1979) who recognized a pattern of centripetal crystallization and accompanying volatile saturation as the paradigm linking the ore suite. In addition, Crocker (1971) noted the existence of silica-iron immiscibility in the mineralization process and also pointed to the link between felsic volcanic activity associated with the BC (i.e. the Rooiberg 'felsites') and pyroclastic-agglomerate-hosted fluorite-hematite mineralization (of the Vergenoeg type) in the latter rocks.

In Figure 12 an attempt has been made to identify the principal styles of polymetallic mineralization associated with the Bushveld granites. Selected as examples are well-studied ore-deposits such as the endogranitic Sn-W mineralization at Zaaipplaats Mine and the exogranitic sediment-hosted Sn-base metal mineralization at the Rooiberg Mine, regarded by Crocker (1979) as end members in the range of ore types observed. For the purpose of this compilation the Cu-Ag-U-F mineralization at the Albert Silver and Spedwell mines is regarded as an additional style of mineralization different but nevertheless genetically related to the granite suite. The characteristics of these deposits are used as the empirical basis to set up a general model which encapsulates many of the characteristics of this metal province. It does *not*, however, take into account the processes that prevailed in the acid extrusives of the Rooiberg Group, where explosive volcanism and brecciation have given rise to fluorite-hematite deposit types which, although probably genetically related, require explanation in terms of processes falling outside the scope of the present study.

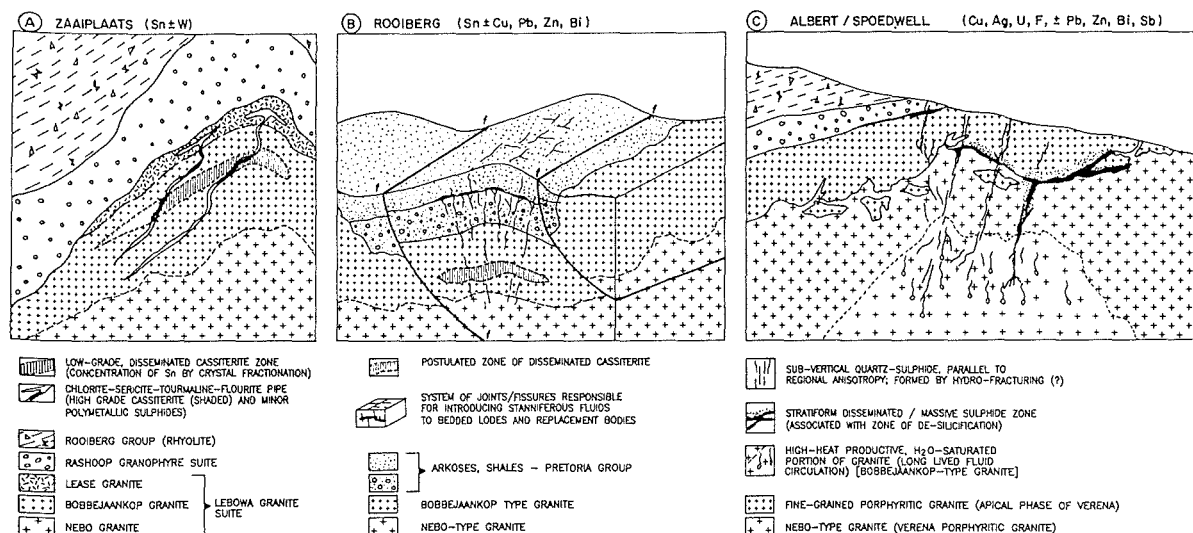


Figure 12: Geological characteristics of the Zaaipplaats-, Rooiberg-, and Albert Silver Mine/Spedwell-styles of mineralization in the Bushveld Complex. Sources of information provided in the text.

Zaaiplaats Mine

Mineralization, consisting of cassiterite, together with scheelite, sulphides and fluorite, at Zaaiplaats is hosted within a coarse-grained hydrothermally altered granite, known locally as the Bobbejaankop Granite, which is capped by a finer-grained, miarolitic roof phase. Two forms of mineralization exist: firstly, a low-grade zone of disseminated cassiterite in the central and upper portions of the Bobbejaankop body, where Sn has been concentrated orthomagmatically by processes akin to Rayleigh Fractionation (Coetzee and Twist, 1989; Groves and McCarthy, 1978), and secondly, in shallow-plunging quartz-sericite-chlorite-tourmaline pipes and lenses generally containing high-grade tin mineralization (Figure 12A; after Crocker, 1986).

Characteristics of the Zaaiplaats mineralization are the wide-ranging fluid temperatures and compositions ($T_h = 600$ to 200°C ; hypersaline to moderate salinity $\text{H}_2\text{O}-\text{NaCl}-\text{CO}_2$), and oxygen isotope signatures ($\delta^{18}\text{O} = 6,5$ to $1,5\%$) (Pollard et al., 1991). In addition, Pb-isotopic studies indicate that isotopic exchange at Zaaiplaats did not cease until circa 1100 Ma ago, indicating an extremely long-lived hydrothermal fluid circulation related to the exceptionally high heat productive capacity of the Bobbejaankop Granite ($25-30 \mu\text{W.m}^{-3}$) (McNaughton et al., 1993). Despite this long-lived activity, which extended hydrothermal activity to relatively low temperatures, incursion of oxygenated meteoric fluids is believed to have been negligible, as confirmed by ^{18}O fluid/rock modelling (Pollard et al., 1991) and the relative paucity of high-level, deeply-penetrating fracture systems. The Zaaiplaats ore body is, therefore, believed to be the result of initial, primary concentration of Sn by crystal fractionation, with later, long-lived, circulation of in-situ derived magmatic fluids which further concentrated Sn into pipe-like conduits.

Rooiberg Mine

Cassiterite and minor chalcopyrite mineralization at Rooiberg is hosted within feldspathic arenites and shales comprising a roof-pendant of the upper Pretoria Group within the Bushveld granites. Two styles of mineralization are evident; firstly, bedding-conformable deposits concentrated within arkosic layers of the Boschoffsberg Quartzite Member, and secondly, fracture-or joint-related lodes. The two styles are often spatially related and comprise identical ore-mineral and alteration paragenesis (Fig. 12B; after Stear, 1977; Rozendaal et al., 1986). The paragenetic sequence of deposition is orthoclase-quartz followed by tourmaline-apatite-cassiterite and, finally, carbonate-chalcopyrite-pyrite (together with minor galena, sphalerite, bismuthinite and gersdorffite) (Leube and Stumpfl, 1963). Detailed fluid characterization of the Rooiberg deposits has not been carried out, although Olilla's (1981) fluid inclusion study documented the presence of predominantly low T_h measurements, in the range $175-220^\circ\text{C}$. A relatively low temperature origin is also suggested by the extremely low Nb contents (15-44 ppm) of cassiterite at Rooiberg (Leube and Stumpfl, 1963). These characteristics are consistent with derivation of Rooiberg mineralization from an original magmatic fluid that migrated some distance from its granitic source, precipitating low-temperature cassiterite and base-metal mineralization in suitable, exogranitic traps represented by roof-zone sediments to the Bushveld granite suite. The predominance of Sn in the Rooiberg paragenesis suggests, as with Zaaiplaats, that hydrothermal fluids may have interacted with a zone of primary cassiterite concentration

formed during progressive crystal fractionation of the subjacent parental granitoid magma (Figure 12B), although there is no direct evidence for such a zone.

Albert Silver/Spoedwell Mines

The Albert Silver and Spoedwell mines differ from the two above examples in that they contain little or no Sn and are dominated by base and precious metals, together with substantial concentrations of hematite -specularite, chlorite, uranium and fluorite. Both deposits occur at the interface between differentiated coarse-grained granites and a fine-grained cap-rock that probably represents a more rapidly crystallized apical facies of the Bushveld granite suite. Mineralization at Spoedwell Mine is dominated by chalcopyrite and pyrite, with minor sphalerite, galena, arsenopyrite and fluorite. Sulphide distribution is markedly stratiform although variably plunging pipe-like alteration zones also occur (Figure 12C; A. Frick personal communication). At ASM mineralization on surface is marked by the presence of a prominent set of sub-parallel gossanous quartz-hematite veins; the degree and extent of stratiform mineralization developed along the coarse-grained - fine-grained granite interface has not been tested and cannot be observed since the old underground workings are flooded.

Although the mineralization at ASM and Spoedwell shows many conceptual similarities to that at Zaaipiaats and Rooiberg, it has some characteristics which are markedly different and, thereby, provide an added variation to the processes of mineralization in the Bushveld granites. Particularly significant is the absence of Sn mineralization, the presence of (lower-temperature) precious metals associated with fahlores, and the existence of a prominent, late-stage, hematite-pitchblende-fluorite-chlorite paragenesis.

The ore paragenetic sequence at ASM comprises early pyrite-chalcopyrite followed by sphalerite-galena and then arsenopyrite and argentiferous tennantite. A similar paragenesis preceded cassiterite precipitation at Zaaipiaats. Fluids at ASM are characterized by a high temperature population (T_h 260-460°C) and compositions are also not dissimilar to those identified at Zaaipiaats (Ollila, 1981). Rb-Sr and Pb-Pb whole-rock isotope systematics at ASM indicate open system behaviour and isotope exchange for long periods subsequent to emplacement of the Bushveld Complex, as is the case for Zaaipiaats and elsewhere. These characteristics are consistent with the notion that mineralization associated with deposits such as ASM and Spoedwell are initiated by magmatic fluids derived after H₂O-saturation within differentiated phases of the Bushveld granites. These fluids were convectively circulated over a lengthy period of geological time as a result of thermal energy supplied by the high heat productive capacity of the most differentiated portions of the granitic suite.

Unlike Zaaipiaats, however, ASM is characterized by a pronounced set of penetrative fractures now filled largely with quartz and specularitic hematite. The Albert Silver Mine, and to a lesser extent Spoedwell, is also characterized by a late assemblage of thuringitic chlorite, hematite, pitchblende and fluorite. In addition, ASM fluids are also characterized by a pronounced low salinity, low T_h (~ 150°C) population which is not apparent at Zaaipiaats. It is suggested that this fluid may have been meteoric in origin, becoming the predominant hydrothermal medium as the magmatic fluid waned. The late Fe-U-F assemblage characteristic of ASM may also have been precipitated by this fluid, which would account for the highly oxidized character of the late paragenesis, and its absence in deposits

where the influence of meteoric fluids has been negligible (i.e. Zaaiplaats). If T_h for the low temperature fluid population at ASM is pressure-corrected for entrapment at 1,5 kb (the depth of formation at Zaaiplaats; Pollard et al., 1991) then trapping temperatures would have been around 240°C. This is broadly comparable with the equilibration temperatures of the ASM chlorites of between 260 - 290 °C (depending on the extent of the Fe/Fe + Mg correction; Table 2) and supports the suggestion that the low temperature fluid observed in ASM fluid inclusions was that associated with precipitation of the later ore paragenesis.

Towards a General Model

Polymetallic metal mineralization in the Bushveld granites, as exemplified by the case of the Zaaiplaats tin deposit, resulted from a high salinity magmatic fluid that interacted with a zone of primary cassiterite concentration formed by crystal fractionation, and was driven by locally derived radiothermal heat that sustained an extremely long-lived fluid convective circulation (Coetzee and Twist, 1989; McNaughton et al., 1993; Pollard et al., 1991). Fluids were largely confined to the upper, apical portions of the Bushveld granite and were trapped at pressures of around 1,5 kb (Pollard et al., 1991) indicating depths of burial of 4-5 km. In cases such as Zaaiplaats, negligible meteoric fluid ingress is recorded, although in many other cases fluids migrated into roof rocks comprising granophyre or Pretoria Group sedimentary roof pendants, causing exogranitic base metal mineralization such as at Rooiberg. Regional differences do, however, exist in terms of the relative abundances of the metal suite, and while the northern and northwestern sectors of the Bushveld granite suite contain numerous tin deposits, the southeastern sector is less well endowed in Sn, but is characterized by a mesothermal Cu-Pb-Zn-Ag paragenesis (e.g. Spodwell/ASM). The reason for this is poorly understood, but may be related to the presence, or otherwise, of primary concentrations of cassiterite in highly differentiated phases such as the Bobbejaankop Granite. In areas where this protore did not form it is likely that hydrothermal activity concentrated a paragenetic association where Sn was not the dominant metal. These characteristics are illustrated and summarized in Figure 13A, which represents the early stages of evolution in the Bushveld polymetallic paragenesis.

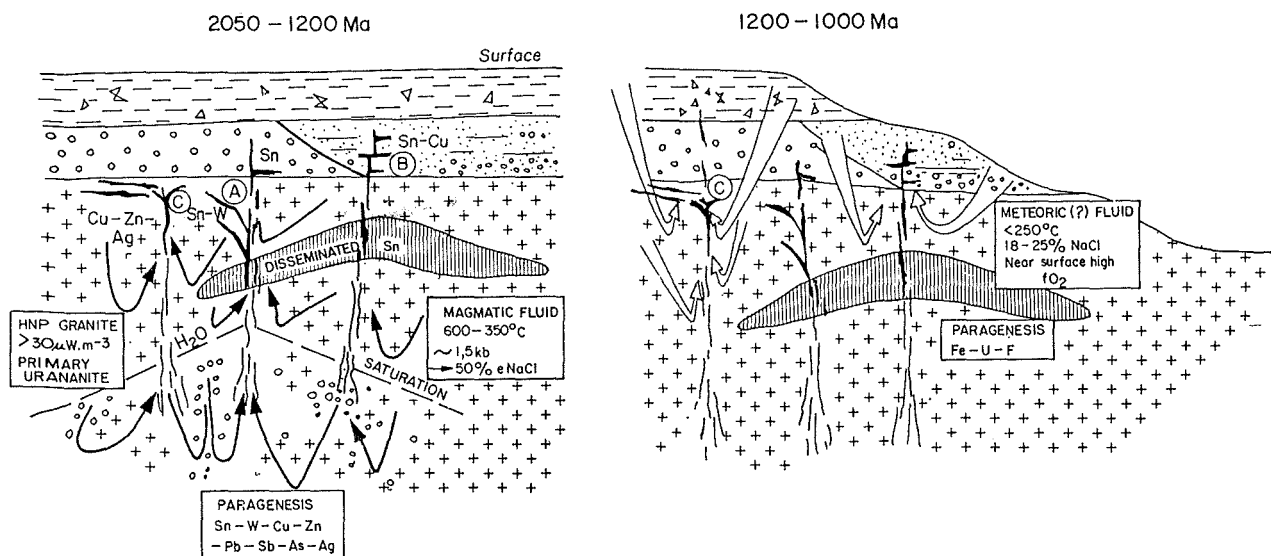


Figure 13: Generalized metallogenic model for polymetallic mineralization in granites of the Bushveld Complex. Description and sources of information are provided in the text.

McNaughton et al. (1993) have suggested that at Zaaiplaats the high heat productive capacity of the Bobbejaankop Granite stimulated fluid convection up until as recently as c. 1100 Ma ago. At this stage, onset of the Namaqua-Natal orogeny resulted in uplift and erosion of the Kaapvaal Craton causing significant cooling of the hydrothermal system, resetting of the U-Pb isotopic system and precipitation of the late stage metal paragenesis. Convective cooling is ruled out for the Bushveld granites and cessation of hydrothermal activity is attributed mainly to an uplift mechanism. In other areas of the Bushveld granite, however, isotopic resetting of both Rb-Sr and U-Pb systems has taken place anywhere between 50 and 500 Ma after emplacement of the suite at 2054 Ma (Walraven and Hattingh, 1993). It is, therefore, clear that variable but pervasive isotope exchange took place in the granite suite particularly in the upper fluid-rich portions, but that cooling (and uplift) took place at different times in different areas. As illustrated in Figure 13B the later stages of Bushveld polymetallic paragenesis were characterized by exhumation of the granite suite, waning of the radiothermally induced magmatic fluid flow, and resetting of the various isotope systems. It is at this stage that incursion of oxygenated meteoric waters was initiated, with the associated development of the late Fe-U-F paragenesis and remobilization of earlier-formed sulphides. It is pertinent to note that development of the late paragenesis, as exemplified by the ASM, only occurs in deposits where well-developed, penetrative fracture systems have formed, and along which significant volumes of meteoric fluid could have passed. Deposits such as Zaaiplaats, where prominent fracture systems are not well-developed, are not characterized by lower temperature base metal parageneses. Consequently, contrasting metal assemblages in the Bushveld granites in deposits which all occur in similar geological settings may, in part, be related to differential uplift rates of the suite and the variable contribution of meteoric fluids into the system. Although this model fits many of the geological characteristics of the polymetallic ore-deposit suite in the Bushveld granites, it still needs to be rigorously tested with detailed fluid inclusion and stable isotope studies.

ACKNOWLEDGEMENTS

This paper is dedicated to the late Dr Louis Coetzee of the Anglo American Corporation, who initiated much of the recent work on the Albert Silver Mine and encouraged the present study. The authors are grateful to Anglo American Prospecting Services and the Atomic Energy Corporation for access to information and financial/logistic support. Dr Derik de Bruijn, Department of Geology, University of the Orange Free State, Bloemfontein, kindly carried out chlorite analyses. Thoughtful reviews by Ian Crocker and Rudi Boer improved the manuscript. Pat King, Lyn Whitfield and Di du Toit kindly typed the manuscript and drafted diagrams.

REFERENCES

- Brown, P.E. and Lamb, W.M., 1989. P-V-T properties of fluids in the system $\text{H}_2\text{O}-\text{CO}_2$ -NaCl: new graphical presentations and implications for fluid inclusion studies. *Geochim. Cosmochim. Acta*, 53, 1209-1221.

- Cathelineau, M. and Neiva, D., 1985. A chlorite solid solution geothermometer. The Los Azufres (Mexico) geothermal system. *Contrib. Mineral. Petrol.*, 91, 235-244.
- Champion, A.T., 1970. *The mineralogy and related geology of the Albert Silver Mine, Bronkhorstspuit, Transvaal*. Unpubl. M.Sc. Dissertation, Univ. Natal, Durban, 96pp.
- Coetzee, J. and Twist, D., 1989. Disseminated tin mineralization in the roof of the Bushveld Granite pluton at the Zaaipplaats Mine, with implications for the genesis of magmatic hydrothermal tin systems. *Econ. Geol.*, 84, 1817-1834.
- Collins, S.D., Beams, S.D., White, A.J.R. and Chappell, B.W., 1982. The nature and origin of A-type granites with particular reference to south-eastern Australia. *Contrib. Mineral. Petrol.*, 80, 189-200.
- Crocker, I.T., 1979. Metallogenic aspects of the Bushveld granites: fluorite, tin and associated rare metal-carbonate mineralization. *Spec. Publ. geol. Soc. S. Afr.*, 5, 275-295.
- Crocker, I.T., 1986. The Zaaipplaats Tinfield, Potgietersrus District. 1287-1299: *In: Anhaeusser, C.R. and Maske, S., Eds. Mineral Deposits of Southern Africa, II*, 2376pp.
- Foster, M.D., 1962. Interpretation of the composition and a classification of the chlorites. *U.S. Geol. Surv. Prof. Pap.*, 414A, 27pp.
- Groves, D. and McCarthy, T.S., 1978. Fractional crystallization and the origin of tin deposits in granitoids. *Mineralium Deposita*, 13, 11-26.
- Kranidiotis, P. and Maclean, W.M., 1987. Systematics of chlorite alteration at the Phelps Dodge massive sulfide deposit, Matagami, Quebec. *Econ. Geol.*, 82, 1898-1911.
- Kleeman, G.J. and Twist, D., 1989. The compositionally-zoned, sheet-like granite pluton of the Bushveld Complex: evidence bearing on the nature of A-type magmatism. *J. Petrol.*, 30, 1383-1414.
- Leube, A. and Stumpfl, E.F., 1963. The Rooiberg and Leeuwpoort tin mines, Transvaal, South Africa. *Econ. Geol.*, 58, 527-557.
- McCarthy, T.S. and Hasty, R.A., 1976. Trace element distribution patterns and their relationship to the crystallization of granite melts. *Geochim. Cosmochim. Acta*, 40, 1351-1358.
- McNaughton, N.J., Pollard, P.J., Groves, D.I. and Taylor, R.G., 1993. A long-lived hydrothermal system in Bushveld Granites at the Zaaipplaats Tin Mine: Lead isotope evidence. *Econ. Geol.*, 80, 27-43.

- Ollila, J.T., 1981. A fluid inclusion and mineralogical study of tin deposits on rocks associated with the Bushveld Complex at the Zaaipplaats, Union and Rooiberg tin mines in the central Transvaal, South Africa. Unpubl. Ph.D. thesis, Rand Afrikaans Univ., Johannesburg, 257pp.
- Pollard, P.J., Andrew, A.S. and Taylor, R.G., 1991. Fluid inclusion and stable isotope evidence for interaction between granites and magmatic hydrothermal fluids during formation of disseminated and pipe style mineralization at the Zaaipplaats tin mine. *Econ. Geol.*, 86, 121-141.
- Rozendaal, A., Toros, M.S. and Anderson, J.R., 1986. The Rooiberg tin deposits, west-central Transvaal, 1307-1328. *In*: Anhaeusser, C.R. and Maske, S., Eds. *Mineral Deposits of Southern Africa*, II, Geol. Soc. S. Afr., 2335pp.
- Stear, W., 1977. The stratabound tin deposits and structure of the Rooiberg fragment. *Trans. Geol. Soc. S. Afr.*, 80, 67-78.
- Taylor, R.P. and Fryer, B.J., 1983. Rare earth element lithogeochemistry of granitoid mineral deposits. *CIM Bulletin*, 76 (860) 74-84.
- Voet, H.W., 1981. Summary of exploration activities, 1885-1980. *Int. Rep. Anglo American Corp. Ltd.*, 14pp.
- Walraven, F., 1981. The Klipkloof Granite of the Bushveld Complex: An example of systematic radiogenic ^{87}Sr loss. *Ann. Geol. Surv. S. Afr.*, 15, 49-53.
- Walraven, F., 1987. Geochronological and isotopic studies of Bushveld Complex rocks from the Fairfield borehole at Moloto, northwest of Pretoria. *S. Afr. J. Geol.*, 90, 352-360.
- Walraven, F. and Hattingh, E. 1993. Geochronology of the Nebo Granite, Bushveld Complex, *S. Afr. J. Geol.*, 96, 31-41.
- Walraven, F., Kleeman, G.J. and Allsopp, H.L., 1985. Disturbance of trace element or isotope systems and its bearing on mineralization in acid rocks of the Bushveld Complex, South Africa. *Conf. High Heat Production Granites (HHP), Hydrothermal Circulation and Ore Genesis*, Instit. Min. Metall., St. Austell, Cornwall, 393-408.
- Walraven, F., Strydom, J.H. and Strydom, N., 1990. Rb-Sr open-system behavior and its application as a pathfinder for Sn mineralization in granites of the Bushveld Complex, South Africa. *J. Geochem. Expl.*, 37, 333-350.

_____oOo_____